Received: 23 October 2023 | Revised: 28 December 2023 | Accepted: 6 January 2024

DOI: 10.1002/psc.3568

RESEARCH ARTICLE

Journal of PeptideScience WILEY

Detailed investigation of the binding abilities of the heterodomain of a multiHis cyclopeptide toward Cu(II) ions

Marco Bortolus[1] | Aleksandra Kotynia[2] | Giacomo Saielli[1,3] | Paolo Ruzza[4] | Marilena Di Valentin[1] | Mauro Carraro[1,3] | Justyna Brasuń[2]

[1]Department of Chemical Sciences, University of Padova, Padova, Italy

[2]Department of Basic Chemical Sciences, Wroclaw Medical University, Wroclaw, Poland

[3]Padova Unit, Institute on Membrane Technology of CNR, Padova, Italy

[4]Padova Unit, Institute of Biomolecular Chemistry of CNR, Padova, Italy

Correspondence
Mauro Carraro, Department of Chemical Sciences, University of Padova, Via Marzolo, 1 – 35131, Padova, Italy.
Email: mauro.carraro@unipd.it

Justyna Brasuń, Department of Basic Chemical Sciences, Wroclaw Medical University, Borowska 211A – 50-556 Wroclaw, Poland.
Email: justyna.brasun@umw.edu.pl

Funding information
Wroclaw Medical University, Poland, Grant/Award Number: SUBZ.DO80.22.024; Department of Chemical Sciences of Padova University, Grant/Award Number: P-DiSC#02BIRD2020; MUR, Grant/Award Number: PRIN2022CAS9ZT

Cyclopeptides hold significant relevance in various fields of science and medicine, due to their unique structural properties and diverse biological activities. Cyclic peptides, characterized by intrinsically higher conformational order, exhibit remarkable stability and resistance to proteolytic degradation, making them attractive candidates for developing targeted drug delivery systems. The aim of this work is to elucidate the unique coordination properties of the multi-His cyclic peptide with c(HDHKHPHHKHHP) sequence (HDCP – heterodomain cyclopeptide). This peptide, indeed, is able to form homo- and hetero-dinuclear complexes in a wide pH range, being thus a good chelator for Cu(II) ions. Herein, we present the results of a combined study, involving potentiometric, spectroscopic (UV–Vis, CD, and EPR), and computational investigations, on its coordination properties. To better understand the interaction pattern with Cu(II) metal ions, two other peptides, each one bearing only one of the two binding domains of HDCP are also considered in this study: c(HDHKHPGGKGGP) = CP1, c(GKGGKPHHKHHP) = CP2, which share sequence fragments of HDCP and allow separate investigations of its coordination domains.

KEYWORDS
CD spectroscopy, copper ion, cyclopeptides, dinuclear complex, potentiometric titration, thermodynamic stability constant, UV–vis spectroscopy

1 | INTRODUCTION

Copper is a significant metal in various biological systems. In particular, it is able to bind to proteins or peptides, being such interactions crucial for Cu transport and storage in many physiological processes. Furthermore, the coordination environment is of utmost importance to regulate its activity in metalloproteins, since it may even result in toxic effects for the cells [1].

One particular group of peptides is that of cyclic peptides, for which the cyclic structure can be formed upon condensation of peptide's residues, e.g. terminal amino and carboxyl (N-C) groups, the amino end and a side chain, the carboxyl end and a side chain, or even between side chains [2]. Cyclization has a stiffening effect on the structure [3] and may allow the peptide to mimic and stabilize the folding or the metal-binding motif of some protein fragments [4, 5].

Cyclic peptides, compared to linear peptides, display [3, 6, 7]:

- longer half-life
- greater resistance to proteases
- higher thermodynamic stability
- higher bioavailability

In addition, their conformational constraints lead, on one hand, to a greater exposed surface area, useful for targeting purposes, and, on

the other hand, to an increased degree of order of the structure, affecting the interaction between metal ions and the amide [8] or side chain donors [9].

The aforementioned Cu-peptide complexes can be designed to simulate the structure and function of different metal enzymes. Due to such properties, tailored peptides can be potentially used as carriers for such metal ions. For example, finding a compound stable in a wide pH range may have a huge impact on the discovery of new treatments involving the chelation and the transfer of copper to a well-defined receptor on the target cell [2]. Moreover, the development of stable copper-based synthetic enzymes (syn-zymes) to be used as catalytic antioxidants in physiological environments still represents a challenging task [10].

Peptide ligands can also find application in medicine, sensing, and environmental remediation [11]. In particular, Cu recovery from electronic wastes [12], may become particularly relevant with the inclusion of copper in the European list of Critical Raw Materials [13]. In this case, the reversible formation of copper complexes would be important to enable copper recycling from composite matrices.

In the present paper, we focus on the detailed analysis of the interactions of the cyclopeptide bearing the c(HDHKHPHHKHHP) sequence (HDCP), toward copper ions. This peptide was designed as a potential structural mimetic of the di-nuclear center of metalloproteins. Besides being rich in donors for copper binding (seven histidine and one aspartic acid residues), the characteristic feature of this ligand is the presence of two proline amino acid residues, which define two potentially independent binding sites. While most of the literature data describe the binding abilities of ligands having two binding domains with the same amino acidic sequence [14, 15], HDCP has two different binding motifs (-*HDHKH*- and -*HHKHH*-) and forms dinuclear complexes in the presence of an excess of metal ions [16]. However, based on the available results, it is still difficult to assess which pocket is preferred by Cu(II) ions and if the binding domains are fully independent. This may be relevant in the case of a low amount of copper or in the presence of different metal ions. Owing to this open question, we present the results obtained for systems with different nL: nCu(II) molar ratios (2:1, 1:1, and 1:2), where L is the HDCP or one of its two analogs with only one of the binding pockets: -*HDHKH*- and -*HHKHH*-, named CP1 and CP2 respectively (Figure 1).

A speciation study has been performed by means of potentiometric titrations, UV–Vis, and circular dichroism (CD) analyses. Additional information on the preferential coordination sites has been collected by electron paramagnetic resonance (EPR) and computational investigations.

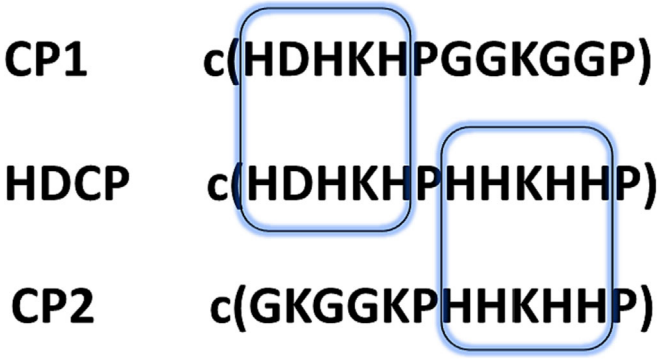

FIGURE 1 Primary structure of the investigated homodetic cyclopeptides CP1, HDCP, and CP2. CP1 and CP2 were specifically designed to maintain one of the two isolated binding motifs of HDCP and both proline breakpoints. The second region in the cyclopeptide was replaced by non-coordinating amino acids (glycine and lysine).

2 | MATERIALS AND METHODS

2.1 | Synthesis

The peptides were prepared by manual SPPS starting from either H-Gly-2Cl-Trt-Resin or H-Asp(OtBu)-2Cl-Trt-Resin. Peptides were assembled using the Fmoc/HBTU chemistry in 0.06-mmolar scale using a three-fold molar excess (0.24 mmol) of Fmoc-amino acids in DMF solution for each coupling cycle. The coupling time was 40 min. Fmoc deprotection was performed with 20% piperidine. N-terminal side chain-protected peptides were obtained by treatment with a 2% trifluoroacetic acid (TFA) solution in DCM (3 × 15 min). After each treatment, the DCM solution was neutralized by the addition of pyridine, and the crude peptides were obtained by the addition of diethyl ether to the concentrated solution. Peptides were cyclized by the addition of diphenyl phosphorazidate (DPPA) (3 eq.) to a 1 mM peptide solution in DMF in the presence of 5 equiv of K_2HPO_4 and stirred at room temperature for 3 days. The DMF solution was concentrated to a small volume and the desired cyclic peptide was precipitated by the addition of water. The crude peptide was obtained after treatment with a TFA/TIS/H_2O (96:2:2, v/v; TIS = triisopropylsilane) solution and precipitation with diethyl ether.

Peptides were purified by HPLC using a Vydac C18, 300 Å, 10 μ, 22 × 250 mm column mounted on a preparative Shimadzu HPLC system (Kyoto, Japan), equipped with LC-8A pumps, SLC-8A controller, SPD-6A spectrophotometric detector, and ERC-3562 ERMA degasser. The column was equilibrated and eluted with the following solvents: (A) 0.05% TFA in H_2O; (B) 0.05% TFA in 9:1 v/v CH_3CN/H_2O; the detector was set at 216 nm and the flow rate was fixed at 12 ml/min. The fractions containing the desired peptide were collected and lyophilized.

The peptides were characterized by LC-ESI-MS analysis, conducted using an Agilent 1,260 Infinity II system equipped with a 6,130 Quadrupole LC–MS analyzer, and the chemical purity of peptides, determined by HPLC, was>95%.

2.2 | Potentiometric titration

The potentiometric measurements were performed on the titration system Titrando 907 (Metrohm), equipped with combined electrode Biotrode®. The electrode calibration was conducted prior each titration to set average electrode parameters (E^0, S_L) according to the equation:

$$E^0 = E + 2.303\frac{RT}{F} log\left[H^+\right] S_L \quad (1)$$

This followed the standard procedure recommended by Irving et al [14, 17]. The samples were prepared by dissolving the powdered ligands in a solution of HCl (3.2×10^{-3} mol/dm^3) and KCl (0.1 mol/dm^3), to get ligand concentrations in the range 5.0–10.0 $\times$ 10^{-4} mol/dm^3, as established by the Gran method [15, 16, 18, 19]. The titrations were carried out in a thermostat glass tube at 298 K in an inert atmosphere and in CO_2-free environment, under Ar gas (5.0). The solutions were prepared by adding equimolar amounts of $CuCl_2$ from stock solutions with final ligand to metals ratios Cu(II)/L = 1:2, 1:1, and 2:1. The titrations were performed, in the pH range 2.5–11.5, using standard KOH 0.1 mol/dm^3 as a titrant.

The potentiometric data allowed to calculate stepwise ($\log K_i$, $\log K_{pqr}$) formation constants by the equations:

$$\log K_i = log\beta_i - log\beta_{(i-1)} \quad (2)$$

$$\log K_{pqr} = log\beta_{pqr} - log\beta_{p(q-1)r} \quad (3)$$

The stoichiometry of complexes and protonation/deprotonation constants ($\beta_i = [H_iL]/[H^+]^i[L]$) of ligand and stability constants ($\beta_{pqr} = [M_pH_qL_r]/[M]^p[H^+]^q[L]^r$) were calculated using HYPERQUAD [17, 20]. In particular, the complexes' distribution diagrams as a function of pH were prepared by the *HySS* (Hyperquad simulation and speciation) program [21].

2.3 | Spectroscopic measurements (UV–Vis and CD)

The samples for UV–Vis and CD experiments were prepared by dissolving the ligands in aqueous HCl/KCl and mixing them with $CuCl_2$ stock solutions to obtain the same ligand-to-metal ratio as in pH-metric titration. The ligand concentration was about 1×10^{-3} mol/dm^3. The collection of spectra was carried out at 298 K as a function of pH at 0.5 unit intervals. The UV–Vis absorption measurements were recorded by a Varian Carry 50 Bio spectrophotometer. All spectra were collected in a quartz cuvette with 1 cm path length. The spectral range was 300–900 nm and the resolution was 0.1 nm. The molar extinction coefficients (ε [M^{-1} cm^{-1}]) were calculated for each spectrum at a wavelength of maximum absorption. The CD spectra were measured on a JASCO J 600 spectropolarimeter in the 220–800 nm range. The optical length of quartz cuvettes was 0.1 or 1 cm. The molar CD coefficient ($\Delta\varepsilon$ [M^{-1} cm^{-1}]) was calculated for each spectrum.

2.4 | EPR measurements

Continuous wave (CW) EPR spectra were recorded on an X band Elexsys E580 spectrometer (Bruker BioSpin GmbH, Rheinstetten, Germany) using a standard rectangular cavity (ER 4102ST) fitted with a cryostat; the temperature was controlled by a liquid nitrogen flow using a variable-temperature controller, Bruker ER4111VT; the microwave frequency was measured by a frequency counter, HP5342A. All the EPR spectra were obtained using the following parameters: microwave power 50 mW, modulation amplitude 0.6 mT, modulation frequency 100 kHz, time constant 82 ms, conversion time 168 ms, scan width 180 mT, 2048 points, and temperature 140 K. All the CW-EPR spectra were obtained in a single scan and checked to ensure the absence of power saturation. They were corrected for the baseline contribution of the cavity by subtraction of the CW-EPR spectrum for the buffer, recorded in the same experimental conditions of the samples. The magnetic field axis was calibrated measuring a DPPH sample. Spectral simulations of CP1 and HDCP were performed using Easyspin version 6.0.0 – dev34 through automated fitting using a combination of Simplex and Levenberg–Marquardt algorithms (*esfit* function) [22]. The fitted parameters were the g-tensor, the hyperfine coupling tensor A, and the linewidths expressed as anisotropic inhomogeneous linewidths through the *HStrain* parameter in the program. For further details see the Supporting Information.

2.5 | Computational studies

A mono-nuclear complex of Cu(II) with the cyclic peptide CP1 was initially built using the software Avogadro [23] and energy was minimized with the UFF Force Field. Using a Density Functional Theory (DFT) approach, the complex was preliminarily optimized at the unrestricted B3LYP (doublet state, considering the unpaired electron in the electronic configuration of Cu(II)) level with 3-21G basis set for H, C, N O and LANL2DZECP for Cu [24]. From the minimized structure, an additional optimization was run using the 6-31G* basis set for all atoms. The solvent reaction field of water was included using the PCM model. Concerning the di-nuclear complexes, four di-nuclear complexes of Cu(II) with the full HDCP cyclic peptide were built and energy minimized using the same protocol above; however, due to the presence of two independent ions, each one with an unpaired electron, the system was kept in the triplet state (as it will be clear from the experimental EPR spectra, no evidence was found concerning the formation of a diamagnetic Cu(II)-Cu(II) pair). Calculations were run using the software package Gaussian 16 [25].

3 | RESULTS AND DISCUSSION

3.1 | The acid/base equilibrium

The characteristic structural feature of the HDCP is the presence of two different and potentially independent Cu(II) binding domains containing the *HDHKH* and *HHKHH* sequences. Both consist of five amino acid residues, of which 3His and 1Asp or 4His motifs, with a high affinity for copper (II). The first studies, performed for HDCP, have shown that in the system with two equivalents of copper (II),

TABLE 1 The calculated protonation constants (β_i) and stepwise constants (K_i) of CP1, CP2, and HDCP were obtained from potentiometric data.

	CP1			CP2			HDCP		
Species	log*β*	log*K*	Amino acid	log*β*	log*K*	Amino acid	log*β*	log*K*	Amino acid
$H_{10}L$							65.36 ± 0.02	2.96	D
H_9L							62.40 ± 0.02	4.73	H
H_8L							57.67 ± 0.02	5.23	H
H_7L				52.40 ± 0.06	3.41	H	52.44 ± 0.03	5.68	H
H_6L	42.16 ± 0.06	3.12	D	48.99 ± 0.06	5.19	H	46.72 ± 0.04	5.81	H
H_5L	39.04 ± 0.05	5.53	H	43.80 ± 0.06	5.94	H	40.91 ± 0.03	6.56	H
H_4L	33.51 ± 0.04	6.19	H	37.86 ± 0.06	6.89	H	34.35 ± 0.03	6.55	H
H_3L	27.32 ± 0.05	7.09	H	30.97 ± 0.05	9.54	K	27.80 ± 0.02	7.67	H
H_2L	20.23 ± 0.03	9.79	K	21.43 ± 0.04	10.27	K	20.13 ± 0.01	9.87	K
HL	10.44 ± 0.04	10.44	K	11.16 ± 0.06	11.16	K	10.26 ± 0.01	10.28	K

the formation of poly-nuclear complexes is preferred (with trinuclear species also appearing around pH 8) [16]. For a detailed investigation of the binding process, the studies of two new analogs of the HDCP are herein presented. CP1 and CP2 have been designed to keep only one metal-binding domain of HDCP: CP1 has in its structure only the *HDHKH* binding domain, whilst CP2 has only the *HHKHH* domain (Figure 1). The remaining part of the peptides only contains glycine and lysine, which are required to keep the same length and a similar backbone, and the proline residues, to define the binding regions.

The potentiometric titration curves allowed to determine the overall (β_i) as well as stepwise (K_i) protonation constants, which have been collected in Table 1. CP1 is characterized by six protonation constants related to the presence of one Asp, three His, and two Lys amino acid residues, while CP2 exhibits seven constants (K_i) assigned to four His and three Lys moieties. The acid–base properties of HDCP were also assessed. The first constant is related to the deprotonation of the side chain carboxyl group of Asp, the next seven to the side chain of His, and the last two constants are related to the side chain of Lys. Such a large number of histidine residues in the structure causes an overlapping of individual species. The log*K* related to the first His dissociation for CP1 and HDCP is higher than that for CP2. This proves that when the peptide sequence contains an Asp residue, the constants of first imidazole deprotonation are usually higher, as was determined in the works on cyclopeptides by Czapor et al. and A. Fragoso et al. [9, 26]. The explanation of this is an intermolecular interaction, through space, between COO^- (Asp) group and the N-H hydrogen atom from the neighboring imidazole ring (His).

3.2 | The copper(II) systems

For a better understanding of the coordination behavior of the HDCP, the binding abilities of the CP1 and CP2 analogs will be described first (see Figure 2A and B, respectively). In the equimolar conditions, in all systems, the coordination process starts above pH 3.0, and the overall and stepwise stability constants are presented in Table 2.

At the beginning of the titration, CP1, with the *HDHKH* domain, loses two and three protons and starts the Cu(II) coordination by sequential formation of the CuH_4L and CuH_3L species. The corrected constant of CuH_4L $\log\beta_4^* = 4.34$ (where $log\beta^* = log\beta_{CuH_nL} - log\beta_{H_nL}$), is similar to the stability constant calculated for the $\{N_{Im}, COO^-\}$ binding mode whilst $\log\beta_3^* = 6.45$ is related to the $\{2N_{Im}, COO^-\}$ coordination manner [27, 28]. Due to the low concentration of these complexes as well as the co-existence of free copper ions and CuH_2L species, it was not possible to obtain the spectroscopic parameters. However, with an increase of pH around 6, CuH_2L is formed as the main species (coordinating, with CuH_3L and CuHL, most of Cu(II)). The stepwise constant (log*K*, Table 2) of the next reaction is 6.67 and corresponds to the deprotonation and binding of the next imidazole nitrogen. Its appearance in the solution significantly influences the spectral properties of the system. The blue shift of the λ_{max} of the d-d band in the UV–Vis spectrum supports the involvement of a third N-donor in Cu(II) binding while the presence of the positive charge transfer (CT) band at 250 nm in the CD spectrum confirms coordination by the imidazole donors (Table 3, Figure 3). There are two possibilities for Cu(II) binding in the CuH_2L complex: $\{3N_{im}, COO^-\}$ or $\{3N_{im}\}$.

To propose the binding mode for the CuH_2L species we have performed theoretical calculations. We should note that the conformational space of these systems is extremely large. The full exploration of the potential energy surface would require molecular dynamic (MD) simulations at a given temperature and within a specific solvent. On the one hand, dealing with complexes with a paramagnetic ion also necessitates either a careful parameterization of a classical force field for the specific case at hand or the use of ab-initio MD simulations. Both approaches are beyond the scope of the present investigation; instead, we aim to answer a more basic question (see also below

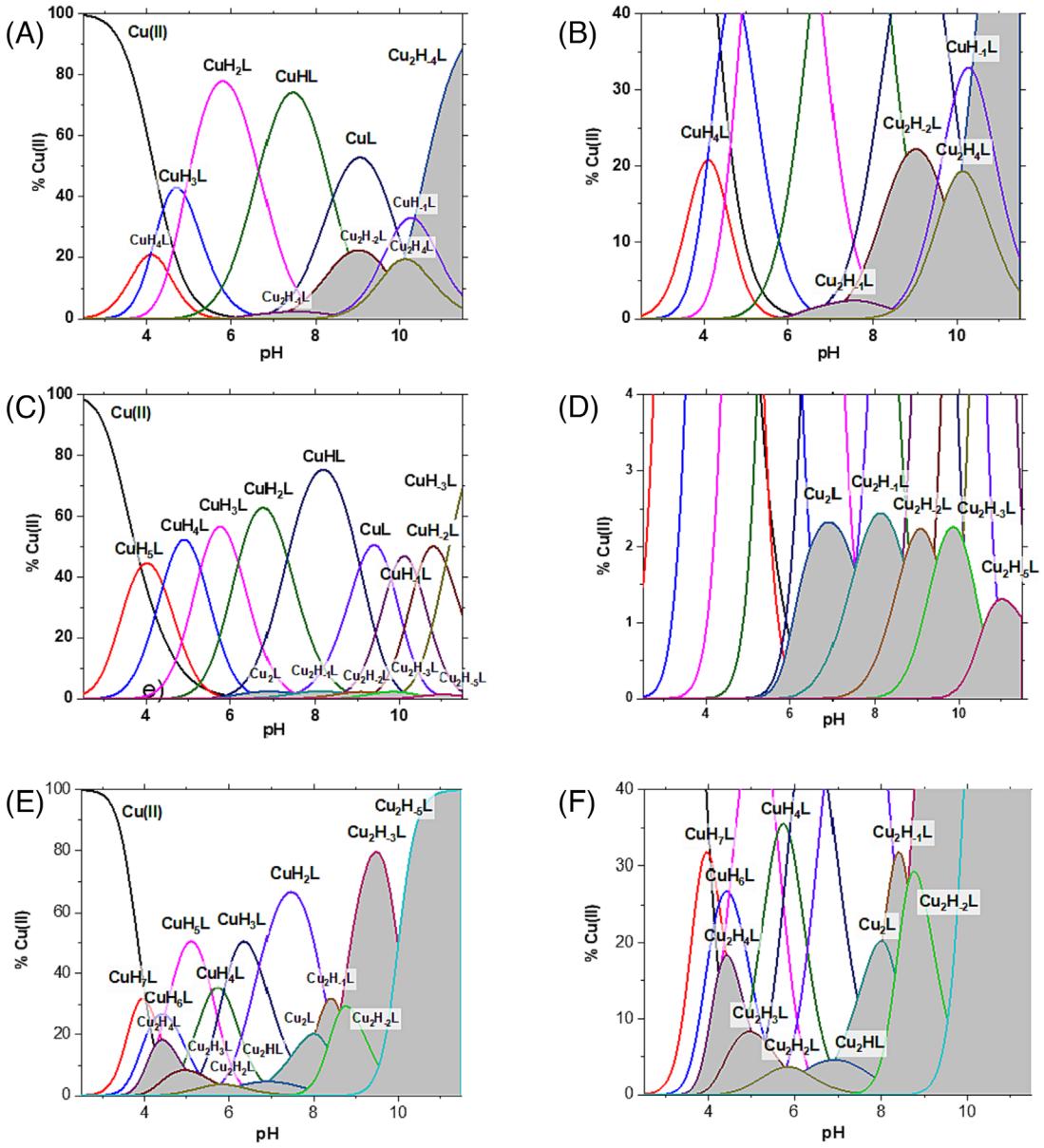

FIGURE 2 The species distribution diagram for Cu(II) complexes in aqueous solution (with zoomed-in panels on the right side): (A,B) L = CP1; (C,D) L = CP2; (E,F) L = HDCP. Experimental conditions: $c_{[L]} = c_{[Cu(II)]} \sim 10^{-3}$ Mol/dm^3, $T = 298$ K, $I = 0.1$ Mol/dm^3, pH range 2.5–11.5.

for the case of the di-nuclear complexes) that is whether such binding modes are plausible or not based on a single point DFT energy minimization.

Firstly, we optimized the structure of the mono-nuclear complex CP1-Cu(II) in the doublet electronic configuration. The initial structure considered copper coordinated by three histidines and two carbonyl oxygens of the peptide backbone. An attempt to bring a carboxyl oxygen close to the copper (II) center (starting distance of 2.2 Å) resulted in a final relaxed structure with the carboxylic group far from the metal (more than 4 Å away, see also Figure S7 with bond distances). We note here that the use of the PCM continuum model as solvent does not allow to consider explicit interactions of the carboxylate with H_2O. Nevertheless, the water molecules would be expected to contrast even more the coordination of Cu(II) with the COO^- group. These results, therefore, suggest that the coordination by the carboxylic group is unlikely to occur due to conformational strain (Figure 3).

In the physiological pH range (around pH = 7.4), CuHL is the dominant species (Figure 2A,B). The location of the λ_{max} for d-d transition at 605 nm is characteristic of the 3N-complex. The previously discussed complex was also 3N-type with λ_{max} for d-d at 630 nm. The blue shift of the λ_{max} supports the replacement of one imidazole by an amide donor as confirmed by the appearance of the negative CT transition at 343 nm in the CD spectrum. The situation started to be more complicated above pH 8 because the di-nuclear species appeared in the system together with the mononuclear complex. However, the spectral features of the system show the presence of the 4N-type complexes with imidazole and amide donors in the internal coordination sphere of the copper (II).

TABLE 2 The calculated log of stability constants (β_i) and stepwise constants (K_i) of Cu(II) complexes with CP1, CP2, and HDCP was obtained from potentiometric data. The experimental conditions were: $c_L \sim 10^{-3}$ Mol/dm^3, $T = 298$ K, $I = 0.1$ Mol/dm^3 (KCl), pH range 2.5–11.0.

	CP1		CP2		HDCP	
Species	logβ	log$K$	logβ	log$K$	logβ	log$K$
CuH_7L	-	-	-	-	57.88 ± 0.04	4.24
CuH_6L	-	-	-	-	53.64 ± 0.06	4.48
CuH_5L	-	-	48.63 ± 0.04	4.40	49.16 ± 0.04	5.59
CuH_4L	37.85 ± 0.07	4.08	44.23 ± 0.04	5.29	43.57 ± 0.05	5.88
CuH_3L	33.77 ± 0.03	4.90	38.94 ± 0.04	6.19	37.69 ± 0.03	6.72
CuH_2L	28.87 ± 0.03	6.67	32.75 ± 0.05	7.34	30.97 ± 0.03	-
CuHL	22.21 ± 0.04	8.40	25.42 ± 0.06	9.05	-	-
CuL	13.80 ± 0.04	9.93	16.36 ± 0.08	9.80	-	-
$CuH_{-1}L$	3.87 ± 0.06	-	6.56 ± 0.08	10.42	-	-
$CuH_{-2}L$	-	-	−3.86 ± 0.09	11.10	-	-
$CuH_{-3}L$	-	-	−15.0 ± 0.1		-	-
Cu_2H_4L	-	-	-	-	48.48 ± 0.05	4.99
Cu_2H_3L	-	-	-	-	43.49 ± 0.04	5.76
Cu_2H_2L	-	-	-	-	37.73 ± 0.05	6.21
Cu_2HL	-	-	-	-	31.52 ± 0.04	6.91
Cu_2L	-	-	23.96 ± 0.05	7.52	24.61 ± 0.04	8.02
$Cu_2H_{-1}L$	13.36 ± 0.05	7.32	16.44 ± 0.07	8.68	16.59 ± 0.05	8.61
$Cu_2H_{-2}L$	6.04 ± 0.06	9.70	7.76 ± 0.08	9.46	7.98 ± 0.06	8.63
$Cu_2H_{-3}L$	−3.65 ± 0.08	10.10	−1.70 ± 0.08	-	−0.65 ± 0.04	-
$Cu_2H_{-4}L$	−13.75 ± 0.06	-	-	-	-	-
$Cu_2H_{-5}L$	-	-	−22.82 ± 0.08	-	−20.64 ± 0.04	-

The CP2 peptide (Figure 2B,C) begins the coordination process by forming CuH_5L as the first complex, which is related to the deprotonation of two imidazole (NH_π) groups. However, the value of log$\beta^* = 4.83$ calculated for this species supports the binding of only one imidazole donor [16, 29–31]. The presence of an imidazole donor in the coordination sphere of Cu(II) is confirmed by the presence of the negative dichroic signal, ascribed to the CT transition, with $\Delta\varepsilon_{302} = -0.51$ in the CD spectrum (Table 3, Figure 4). At pH 5.0, the next species, CuH_4L, reaches its highest concentration. The log$\beta^* = 6.37$ is characteristic for $\{2N_{im}\}$ complexes [27, 29]. The involvement of the second imidazole donor causes an increase in the CT transition intensity, $\Delta\varepsilon_{297} = -0.95$. With the increase of pH, the next form, CuH_3L, appears. The constant log$K = 5.19$ for the reaction $CuH_4L \leftrightarrow CuH_3L + H^+$ is comparable to the log$K = 5.29$ calculated for the fourth His in the free ligand that supports deprotonations without any change in the coordination sphere of the metal ion.

Further deprotonation leads to the appearance of CuH_2L, which dominates at pH 6.9. The value of log$K = 6.19$ may be assigned to the deprotonation of the first peptidic nitrogen and its coordination with Cu(II) ion. This process is well supported by the appearance of a new negative band with $\Delta\varepsilon_{340} = -0.57$ in the CD spectrum (Table 3, Figure 4). Moreover, the location of the d-d transition at 595 nm in UV–Vis spectrum strongly supports 3N-type coordination, in agreement with the theoretical λ_{max} calculated for $2N_{im}$, N^-, H_2O chromophores located in the plane [23, 26]. With the formation of the next species, CuH_1L, some changes in the absorption spectra are observed. The $\lambda_{max} = 575$ nm is still typical for 3N-type complexes, but the blue shift supports the presence of stronger donors in the coordination sphere of the metal ion. This change may be assigned to the replacement of one imidazole donor by an amide and the formed complex may be described by the $\{N_{im}, 2\ N^-\}$ coordination mode [26]. Above pH 9, the next four dominant species, CuL, $CuH_{-1}L$, $CuH_{-2}L$, and $CuH_{-3}L$, appear in the solution. The spectroscopic parameters obtained at pH 11.30 describe the final $CuH_{-3}L$ complex and show a $\{N_{im}, 3\ N^-\}$ coordination manner.

Initially, HDCP creates only mononuclear complexes (Figure 2E,F). The CuH_7L and CuH_6L complexes appear as the first with the values of the corrected stability constants, log$\beta^* = 5.44$ for CuH_7L and log$\beta^* = 6.94$ for CuH_6L. The value of logβ^*_{CuH6} is close to the logβ^* found for CuH_3L of CP1 supporting the same coordination model, $\{2N_{im}, COO^-\}$. The CuH_5L is the dominant mononuclear form that achieves its highest concentration at pH 5.0. The CD spectrum indicates the involvement of only imidazole nitrogen donors in the coordination of the copper(II) ion. This is confirmed by the presence of two $CT_{Nim \rightarrow Cu(II)}$ bands with $\Delta\varepsilon_{320} = 0.34$ and $\Delta\varepsilon_{250} = 4.38$ (Table 3, Figure 4). In addition, the value of log$\beta^* = 8.27$ is close to the value for the CuH_2L complex of CP1 (log$\beta^* = 8.64$) with three imidazole donors involved in Cu(II) binding. With the increase of pH in the system, two co-existing species, CuH_4L and CuH_3L, appear in

TABLE 3 The spectroscopic data of equimolar systems for CP1, CP2, HDCP ligands. The experimental conditions were L to Cu(II) ratio = 1:1.

	Prevalent			UV–Vis		CD	
Ligand	Species	Donor atoms	pH	λ [nm]	ε [M^{-1} cm^{-1}]	λ [nm]	ε [M^{-1} cm^{-1}]
CP1	CuH_3L	{$2N_{im}$, COO^-_{Asp}}	4.50	680[a]	20	-	-
	CuH_2L	{$3N_{im}$}	5.80	630[a]	53	258[b]	0.73
	CuHL	{$2N_{im}$,N^-}	7.25	605[a]	68	515[a]	0.18
						343[c]	−0.59
						279 sh	
						250[b]	2.47
	CuL	{N_{im},2 N^-}	9.0	580[a]	70	515[a]	0.25
						343[c]	−1.09
						280 sh	
						250[b]	4.14
	$Cu_2H_{-4}L$		11.40	540[a]	77	617[a]	0.34
						503[a]	−0.11
						340[c]	−0.44
						250[b]	3.34
CP2	CuH_5L	{N_{im}}	4.0	650[a]	24	620[a]	0.15
						302[b]	−0.51
	CuH_4L	{$2N_{im}$}	5.0	646[a]	42	620[a]	0.23
						302[b]	−0.93
	CuH_2L	{$2N_{im}$,N^-}	7.0	595[a]	60	632[a]	0.20
						535[a]	−0.07
						340[c]	−0.57
						257[b]	1.44
	CuHL	{N_{im},2 N^-}	8.14	575[a]	75	632[a]	0.29
						535[a]	−0.18
						345[c]	−0.78
						257[b]	3.11
	$CuH_{-1}L$	{N_{im},3 N^-}	10.0	540[a]	86	630[a]	0.60
				594 sh		502[a]	−0.57
						355[c]	−0.25
						316[c]	0.47
						258[b]	4.06
	$CuH_{-3}L$	{N_{im},3 N^-}	11.30	530[a]	104	630_a	0.75
				594 sh		502_a	−0.95
						323_c	0.73
						258[b]	4.29
HDCP	CuH_6L		4.50	608[a]	40	-	-
	CuH_5L		5.0	594[a]	44	670[a]	0.16
						545[a]	−0.48
						320[a]	0.34
						250[b]	4.38
	CuH_2L		7.10	580[a]	52	670[a]	0.23
						545[a]	−0.63
						320[b]	0.44
						250[b]	5.35
	$Cu_2H_{-3}L$		9.0	553[a]	70	622[a]	0.49

(Continues)

TABLE 3 (Continued)

Ligand	Prevalent			UV–Vis		CD	
	Species	Donor atoms	pH	λ [nm]	ε [M^{-1} cm^{-1}]	λ [nm]	ε [M^{-1} cm^{-1}]
				608 sh		522[a]	−0.26
						340[c]	−0.36
						253[b]	3.50
	$Cu_2H_{-5}L$		11.0	534[a]	74	622[a]	0.71
				608 sh		503[a]	−0.59
						320[c]	0.42
						255[b]	3.85

[a]d-d transition.
[b]NIm → Cu(II) CT transition.
[c]Namide → Cu(II) CT transition.

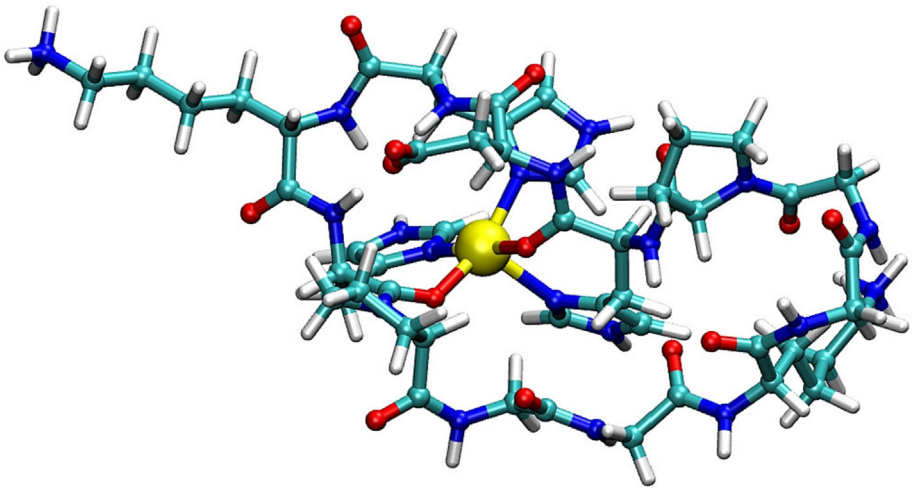

FIGURE 3 The optimized structure of the CuH_2L complex. Cu: yellow, N: blue, C: cyan, O: red, H: white. A closer view of Cu(II) coordination sphere, with selected distances, can be found in Figure S7.

solution. In the pH range from 5.5 to 6.5, the maximum peak at 580 nm was detected in the absorption spectrum, which is consistent with the theoretical Prenesti equation [29, 32] for the $\{4N_{im}\}$ in square planar symmetry complex. In addition, similar spectroscopic parameters were determined for $\{4N_{im}\}$ mode of the previously published cyclopeptides: c(HKHPHKHP) and c(GHKHGPGHKHGP) [14, 33]. The corrected stability constants ($log\beta^*_{CuH_xL} = log\beta_{CuH_xL} - log\beta_{H_xL}$) for CuH_4L and CuH_3L are respectively 9.23 and 9.90 and indicate coordination of the Cu(II) ion by four nitrogen donors from the side chains of His residues [9, 31]. The next equilibrium $[CuH_3L] \leftrightarrow [CuH_2L] + H^+$ ($\log K = 6.64$) indicates proton dissociation from the imidazole ring of the last His residue. The spectroscopic properties are the same, so this process does not influence the coordination motif of the metal ion.

Surprisingly, even if the system is equimolar, dinuclear complexes are dominant with the final $Cu_2H_{-5}L$ above pH 8. The analysis of the spectroscopic parameters supports the same, $\{2N_{Im}, 2N^-_{am}\}$ $\{N_{Im}, 3N^-_{am}\}$, binding mode found for the complexes with the same stoichiometry formed in the system with double excess of Cu(II) [16].

As it was presented above, HDCP starts copper(II) binding by its anchoring to the domain with the *HDHKH* sequence. Below pH 8, mononuclear complexes dominate with only imidazole donors involved in copper(II) coordination, whilst above this pH mainly di-nuclear species exist as it was observed in the system with a double excess of Cu(II) ions. Owing to these facts, the analysis of the pH-dependent EPR spectra was performed for the following systems: nCP1/nCu(II) = 1:1, nHDCP/nCu(II) = 1:1 and nHDCP/nCu(II) = 1:2; the full array of EPR spectra is reported in the Supporting Information, while Figure 5 reports a selection. The EPR simulation parameters were obtained by fitting the filtered spectra for each pH using Easyspin [22], as detailed in the Supporting Information. Selected parameters are presented in Table 4.

All EPR spectra are consistent with a square planar (or elongated octahedral) coordination of copper; however, at neutral pH and above, the g-tensor is rhombic suggesting that the geometry of the planar ligands is distorted. The distortion, however, is not sufficient to support a tetrahedral or trigonal bipyramidal coordination geometry, that would lead to a different symmetry of the tensor altogether (these observations are confirmed by the calculations, see below). The EPR parameters obtained around pH 5.1 for the $HDCP_{1:1}$ support the binding of three nitrogen donors to the metal ion, as observed for the CP1. Then, with the increase of pH, an increase of the $A_{||}$and a

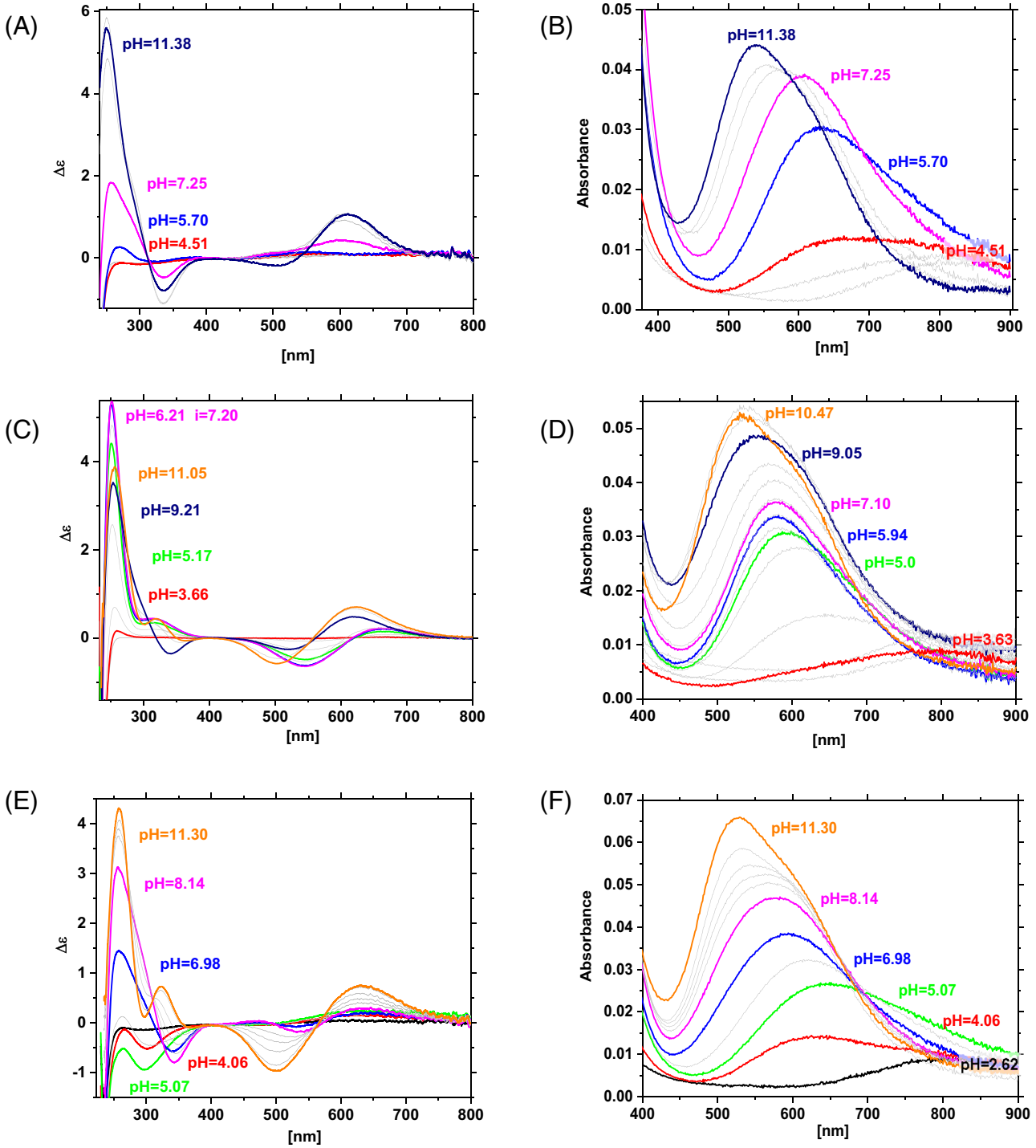

FIGURE 4 The pH dependence of the CD (left) and the UV–vis (right) spectra of Cu(II) systems for CP1 (A,B), CP2 (C,D), and HDCP (E,F). The experiment conditions were: $c_L \sim 10^{-3}$ Mol/dm^3, and the ligand-to-metal ratio was 1.0:0.9.

concomitant decrease of $g_{||}$are observed for $HDCP_{1:1}$ and $HDCP_{1:2}$ The $A_{||} \approx 197$ G and $g_{||} = 2.25$ are characteristic for the complexes with the $\{4N_{Im}\}$. Such observation strongly supports the existence of the same complex in both systems (Table 4). The slightly broader lineshapes that can be observed at a 2:1 Cu(II):peptide ratio (Figure 5), suggest that the copper ions interact only via a moderate dipolar interaction and are neither diamagnetically coupled ($S = 0$), which would imply no EPR spectrum, nor strongly ferromagnetically coupled, which would lead to a completely different lineshape.

The investigated HDCP, independently from the ligand-to-metal molar ratio prefers the formation of the final dinuclear, $Cu_2H_{-5}L$, complex. The formation of this species is related to the dissociation of five amide protons and is described as $\{2N_{Im}, 2N^-_{am}\}$ $\{N_{Im}, 3N^-_{am}\}$. Since HDCP consists of two different binding domains, there are few

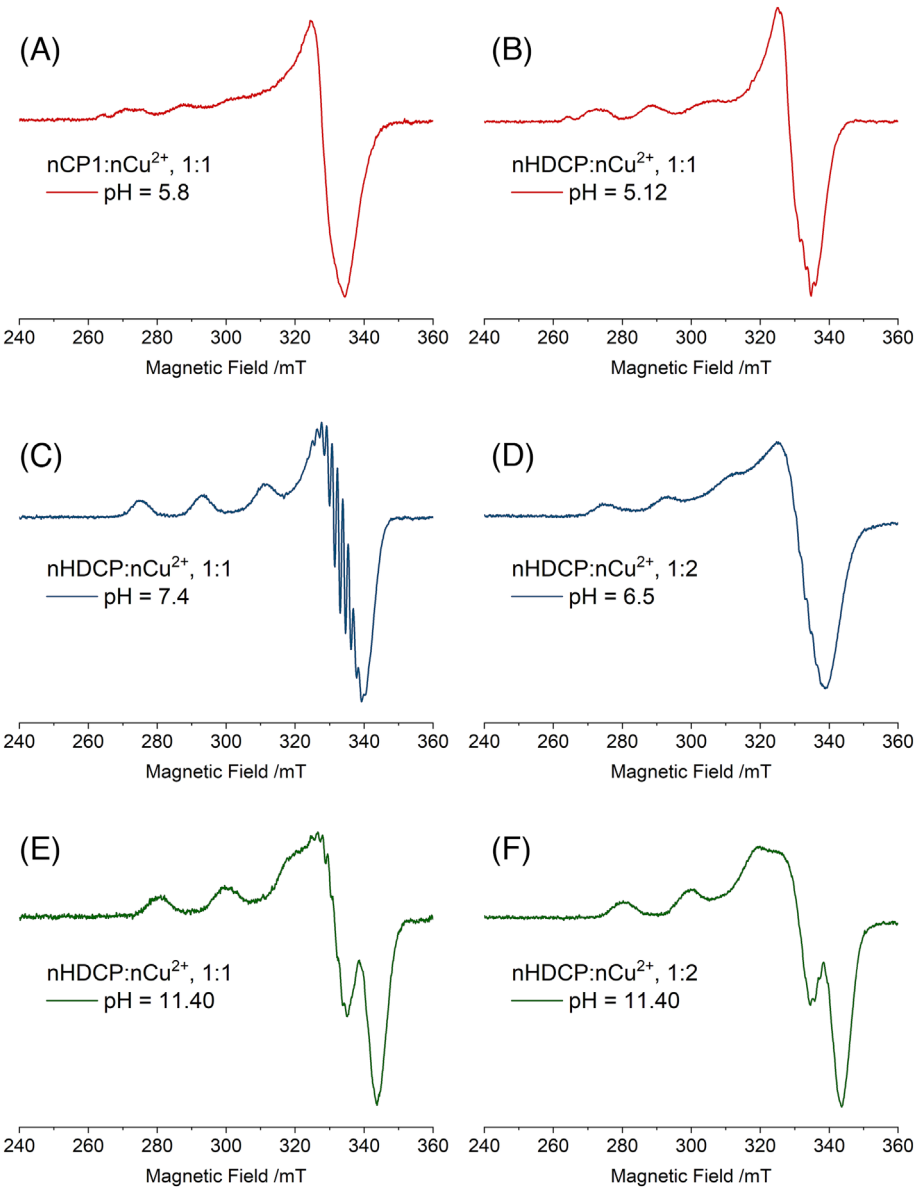

FIGURE 5 Selected X-band CW-EPR spectra of Cu(II) complexed by CP1 or HDCP at different pH values and molar ratios (T = 140 K). Colors are the same as those used in Table 4. (A) nCP1/nCu(II) = 1:1, pH = 5.8; (B) nHDCP/nCu(II) = 1:1, pH = 5.12; (C) nHDCP/nCu(II) = 1:1, pH = 7.4; (D) nHDCP/nCu(II) = 1:2, pH = 6.5; (E) nHDCP/nCu(II) = 1:1, pH = 11.40; (F) nHDCP/:nCu(II) = 1:2, pH = 11.40.

TABLE 4 The EPR parameters, $A_{||}$component of the A tensor (± 5 G) and g tensor (± 0.001), for copper(II) complexes for CP1 and HDCP. Parameters in bold refer to the spectra in Figure 5 (same color key). When the numbers are reported in italics, the main species is the same as the one not in italics.

nCP1/nCu(II) = 1:1					**nHDCP/nCu(II) = 1:1**					**nHDCP/nCu(II) = 1:2**				
pH	**$A_{||}$ (G)**	**g_{xx}**	**g_{yy}**	**g_{zz}**	**pH**	**$A_{||}$ (G)**	**g_{xx}**	**g_{yy}**	**g_{zz}**	**pH**	**$A_{||}$ (G)**	**g_{xx}**	**g_{yy}**	**g_{zz}**
5.8	**171**	**2.063**	**2.067**	**2.314**	**5.12**	**184**	**2.053**	**2.071**	**2.295**	-	-	-	-	-
-	-	-	-	-	6.30	195	2.047	2.078	2.258	**6.5**	**197**	**2.035**	**2.070**	**2.255**
7.25	*	*	*	*	7.40	199	2.052	2.055	2.256	-	-	-	-	-
8.80	*207*	*2.049*	*2.086*	*2.204*	8.90	195	2.047	2.062	2.254	8.34	*207*	*2.042*	*2.070*	*2.202*
10.24	*207*	*2.049*	*2.086*	*2.204*	9.80	206	2.044	2.071	2.212	9.36	*207*	*2.042*	*2.070*	*2.202*
11.46	207	2.049	2.086	2.204	11.40	209	2.038	2.066	2.204	11.40	207	2.042	2.070	2.202

*Multicomponent spectrum.

possibilities for metal ions binding. Due to this fact, the preliminary theoretical calculations were performed for the four most likely sets of nitrogen donor atoms involved in the Cu(II) binding in the $Cu_2H_{-5}L$ complex (Figure 6).

As mentioned already above, rather than trying to explore the full conformational space, the calculations were aimed at checking if the idea of two independent binding sites in the HDCP cyclopeptide, which are supposed to be the same as the single binding sites in the CP1 and CP2, respectively, was plausible or not, plus obtaining some structural information concerning the structure of the coordination sphere of Cu(II).

The electronic energies of the energy-minimized structures are in the order tL > > tR > bL > bR, see Table 5. It seems, therefore, unlikely that the true structure is tL, while the other three have relatively close energies, and DFT calculations of such large systems with a complex conformational potential energy surface do not allow to state with confidence which is the most probable structure in solution.

A key feature, however, that we can observe in the minimized geometries in all cases is a non-perfect square planar geometry around the Cu(II) center, likely due to a conformational strain of the peptide chain. In Table 5 we also report the N-Cu-N angles for each metal center of the dinuclear complex, labeled Cu_a (the copper on the blue half of the peptide) and Cu_b (the copper on the green side). The two nitrogens used to define the angle are the pairs in opposite positions, so there are two such angles for each metal center. These angles would be both 180° for a perfect square planar geometry.

As we can see, there are about 30–40 degrees of deviation from a square planar geometry for all metal centers in the four structures investigated. As an example, the structure of the conformer bR is shown in Figure 7.

In Figure S8 we also show the spin density of the HDCP complex of Figure 7 (bR conformer): although the system is assumed to be in a triplet state during the DFT calculations, it is clear that there is no significant overlap between the spin densities of the two Cu(II) ions, therefore supporting the idea of the two independent binding sites being the same as in the CP1 and CP2 cyclopeptides.

Moreover, we attempted to coordinate both Cu(II) metal centers by two water molecules, placed roughly on the top and bottom with respect to the average plane defined by the distorted square planar coordination. The optimization in this case was run with the smaller

TABLE 5 The N-Cu-N angles for each metal center of the dinuclear complex are labeled Cu_a (the copper on the blue half of the peptide, Figure 6) and Cu_b (the copper on the green side, Figure 6).

	Energy (kcal/Mol)	N-Cu_a(II)-N (°)	N-Cu_b(II)-N (°)
tL	25.6	144.6; 145.0	141.6; 151.7
tR	4.3	148.4; 141.5	150.6; 141.9
bL	2.2	155.4; 158.5	138.9; 145.4
bR	0.0	148.9; 169.7	139.4; 151.6

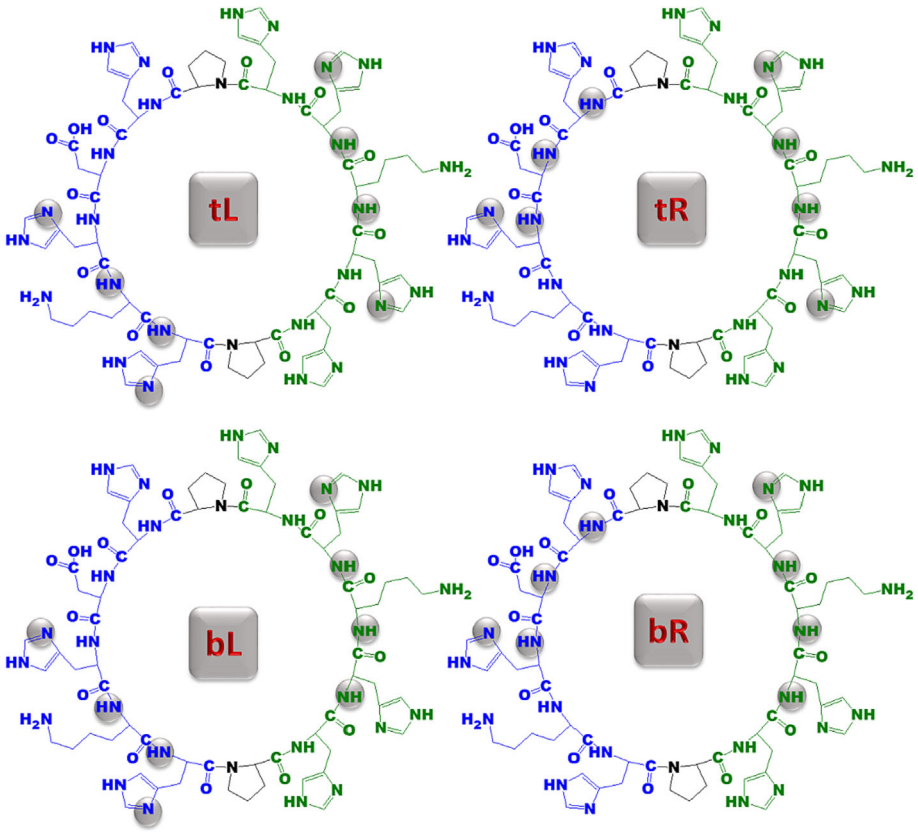

FIGURE 6 The different sets of nitrogen donor atoms involved in the Cu(II) binding in the $Cu_2H_{-5}L$ complex, tL = top left, tR = top right, bL = bottom left, bL = bottom right simply refer to the position in the figure.

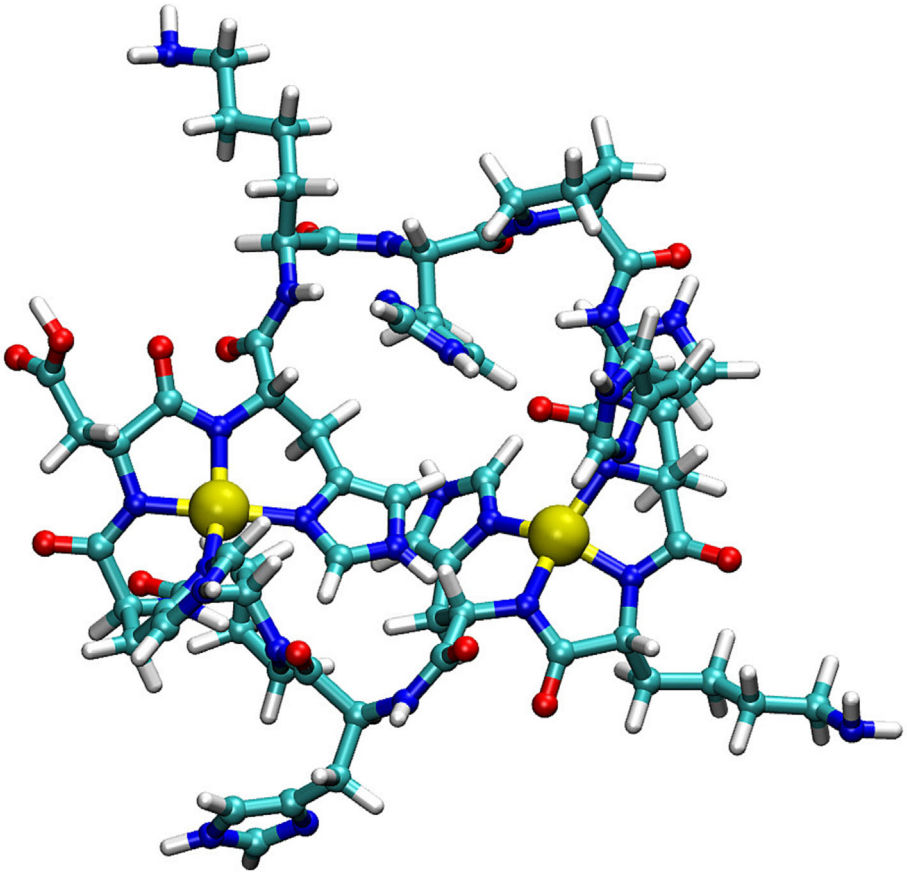

FIGURE 7 The proposed optimized structure of the conformer bR. Cu: yellow, N: blue, C: cyan, O: red, H: white.

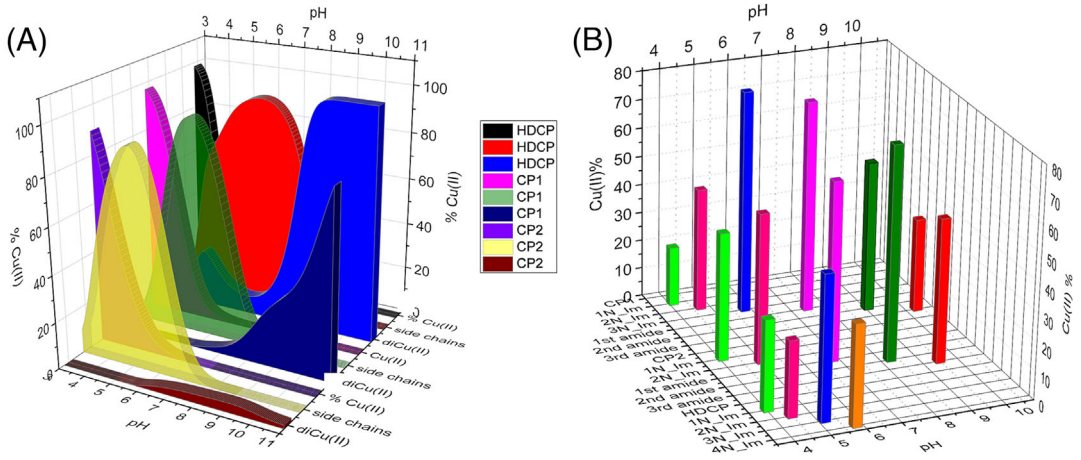

FIGURE 8 (A) Effect of pH on the formation of complexes with the three peptides CP1, CP2, and HDCP. Cu(II): free copper; side chains: Cu(II) complexes with only side chain donors; diCu(II): dinuclear complexes; (B) donors involved in the formation of copper complexes with CP1, CP2, and HDCP, for nL/nCu(II) = 1:1, at different pH. The colored bars represent the amount of copper coordinated by the following donors: light green: $1N_{Im}$; dark pink: $2N_{Im}$; blue: $3N_{Im}$; orange: $4N_{Im}$; magenta: 1st amide; dark green: 2nd amide; red: 3rd amide.

basis set. In all four cases, we did not observe any coordination in the final energy-minimized structures, since all water molecules were involved in H-bonds with the groups of the peptide chain and driven far away from the metal center.

In order to underline the different behavior of the peptides, we can focus the attention on the analyses carried out for the systems with nL/nCu(II) = 1:1 M ratio.

Figure 8A shows the comparison of the formation of the mononuclear complexes, with the involvement of only side chain donors, and dinuclear complexes of CP1, CP2, and HDCP. As it was shown above, all systems can form dinuclear complexes. The tendency to them increases in the order CP2 < < CP1 < HDCP (Figure 8A). This difference may be caused by the increased number of side chain groups that are able to bind one Cu(II) ion in the same complex (CP2:

two groups - $2N_{Im}$, CP1: three groups - $2N_{Im}$ and $-COO^-$ or $3N_{Im}$, HDCP: four groups – $4N_{Im}$).

CP1 and CP2 form mononuclear complexes with only side chain donors {$1N_{Im}$, $2N_{Im}$, $3N_{Im}$} between pH 3 and 7, whilst the presence of seven His amino acid residues in HDCP favors mononuclear complexes with only side chains donors, with the additional {$4N_{Im}$}, up to pH 6 (Figure 8A,B). The involvement of the first imidazole donor {$1N_{Im}$}, is observed almost at the same pH for all investigated peptides (Figure 8B). The participation of the carboxylate group in the metal binding by the CP1 peptide favors the formation of the complex with the {$3N_{Im}$} binding mode, observed around pH 6 (Figure 8B). For what concerns amide donors, the comparison between CP1 and CP2 shows that the latter forms these complexes, involving first, second, and third amides, at a significantly lower pH range. On the other hand, HDCP does not form mononuclear complexes with the peptidic donors, since above pH 7.5 it forms only dinuclear species.

4 | CONCLUSION

In this manuscript, we describe the results of potentiometric and spectroscopic studies on the coordination properties of cyclopeptides with Cu(II) ions. Our research involved a multiple approach to get a better understanding of the interaction between Cu(II) ions and the peptides under investigation. The main objective of the study was to investigate the coordination properties of multi-His cyclopeptides. It has been shown that in a system with two copper(II) equiv, multinuclear complexes are easier to form. On the other hand, at pH below 8, mononuclear complexes predominate.

Our results may inspire the development of novel biomimetic systems for various biological, medical, and environmental applications. Tailored cyclic peptides, indeed, could be designed with a wide range of structural motifs, to tune the interaction with metal ions. Cyclic peptides designed for copper binding can serve as valuable tools to mimic natural copper-binding sites in proteins and enzymes, aiding the understanding of copper's role in vital cellular processes. Furthermore, these peptides hold promise in developing therapies for copper-related diseases, such as certain neurodegenerative disorders, by helping to manage copper levels within the body or to devise new catalytic antioxidants [10, 34, 35].

ACKNOWLEDGEMENTS

This research was funded by Wroclaw Medical University, Poland, grant number SUBZ.DO80.22.024, by the Department of Chemical Sciences of Padova University (P-DiSC#02BIRD2020 project) and MUR (PRIN2022CAS9ZT). DFT calculations were run on the C3P Linux cluster of the Department of Chemical Sciences of the University of Padova. JB would like to thank students Paulina Świątek and Filip Dębicki for all their assistance in the preparation of this publication.

CONFLICT OF INTEREST STATEMENT

The authors declare no conflict of interest.

ORCID

Mauro Carraro https://orcid.org/0000-0002-1194-6147

REFERENCES

1. Kozlowski H, Janicka-Klos A, Brasun J, Gaggelli E, Valensin D, Valensin G. Copper, iron, and zinc ions homeostasis and their role in neurodegenerative disorders (metal uptake, transport, distribution and regulation). *Coord Chem Rev*. 2009;253:2665-2685. doi:10.1016/j.ccr.2009.05.011
2. Jensen KJ. *Peptide and protein design for biopharmaceutical applications*. Wiley; 2009.
3. Bockus AT, McEwen CM, Lokey RS. Form and function in cyclic peptide natural products: a pharmacokinetic perspective. *Curr Top Med Chem*. 2013;13:821-836. doi:10.2174/1568026611313070005
4. Bong DT, Clark TD, Granja JR, Ghadiri MR. Self-assembling organic nanotubes. *Angew Chem Int Ed*. 2001;40:988-1011. doi:10.1002/1521-3773(20010316)40:6%3C988::AID-ANIE9880%3E3.0.CO;2-N
5. Hartgerink JD, Granja JR, Milligan RA, Ghadiri MR. Self-assembling peptide nanotubes. *J Am Chem Soc*. 1996;118:43-50. doi:10.1021/ja953070s
6. Hruby VJ, al-Obeidi F, Kazmierski W. Emerging approaches in the molecular design of receptor-selective peptide ligands: conformational, topographical and dynamic considerations. *Biochem J*. 1990;268(2):249-262. doi:10.1042/bj2680249
7. Rovero P. *Solid-phase synthesis*. New York, NY; 2000:331-364.
8. Bal W, Kozlowski H, Lammek B, Rolka K, Pettit LD. Potentiometric and spectroscopic studies of the Cu (II) complexes of Ala-Arg8-vasopressin and oxytocin: Two vasopressin-like peptides. *J Inorg Biochem*. 1992;45:193-202. doi:10.1016/0162-0134(92)80044-V
9. Czapor H, Bielińska S, Kamysz W, Szyrwiel Ł, Brasuń J. The cyclopeptides with the multi-His motif as ligands for copper (II). *J Inorg Biochem*. 2011;105:297-302. doi:10.1016/j.jinorgbio.2010.11.011
10. Squarcina A, Santoro A, Hickey N, et al. Neutralization of reactive oxygen species at dinuclear Cu (II)-Cores: tuning the antioxidant manifold in water by ligand design. *ACS Catal*. 2020;10:7295-7306. doi:10.1021/acscatal.0c01955
11. Bassan GA, Marchesan S. Peptide-based materials that exploit metal coordination. *Int J Mol Sci*. 2023;24(1):456. doi:10.3390/ijms24010456
12. Zhang J, Zhang X, Wang R, et al. Copper recovery from waste printed circuit boards with small peptides enhanced by ultrasound. *Sep Purif Technol*. 2023;315:123680. doi:10.1016/j.seppur.2023.123680
13. European Critical Raw Materials Act. *Proposal for a regulation of the European Parliament and of the council establishing a framework for ensuring a secure and sustainable supply of critical raw materials and amending regulations (EU) 168/2013, (EU) 2018/858, 2018/1724 and (EU) 2019/102*. COM(2023) 160, SWD(2023) 160, SWD(2023) 161, SWD(2023) 162, SEC(2023) 360.
14. Kotynia A, Czyżnikowska Ż, Bielińska S, et al. The impact of two–Gly-ProGly–motifs on formation of di-copper complexes by His 4-cyclopeptides. *New J Chem*. 2014;38:5198-5206. doi:10.1039/C4NJ00689E
15. Kotynia A, Janek T, Czyżnikowska Ż, Bielińska S, Kamysz W, Brasuń J. The analysis of cu(II)/Zn(II) Cyclopeptide system as potential cu, ZnSOD mimic center. *Int J Pept Res Ther*. 2017;23(4):431-439. doi:10.1007/s10989-017-9574-8
16. Kotynia A, Marciniak A, Brasuń J. The formation of di-copper (II) complexes with a hetero-site cyclopeptide–spectroscopic and potentiometric studies. *Polyhedron*. 2020;185:114585. doi:10.1016/j.poly.2020.114585
17. Irving HM, Miles MG, Pettit LD. A study of some problems in determining the stoicheiometric proton dissociation constants of complexes by potentiometric titrations using a glass electrode. *Anal Chim Acta*. 1967;38:475-488. doi:10.1016/S0003-2670(01)80616-4

18. Gran G. Determination of the equivalence point in potentiometric titrations. Part II. *Analyst*. 1952;77:661. doi:10.1039/AN9527700661
19. Gran G, Dahlenborg H, Laurell S, Rottenberg M. Determination of the equivalent point in potentiometric titrations. *Acta Chem Scand*. 1950; 4:559-577. doi:10.3891/acta.chem.scand.04-0559
20. Gans P, Sabatini A, Vacca A. Investigation of equilibria in solution. Determination of equilibrium constants with the HYPERQUAD suite of programs. *Talanta*. 1996;43(10):1739-1753. doi:10.1016/0039-9140(96)01958-3
21. Alderighi L, Gans P, Ienco A, Peters D, Sabatini A, Vacca A. Hyperquad simulation and speciation (HySS): a utility program for the investigation of equilibria involving soluble and partially soluble species. *Coord Chem Rev*. 1999;184:311-318. doi:10.1016/S0010-8545(98)00260-4
22. Stoll S, Schweiger A. EasySpin, a comprehensive software package for spectral simulation and analysis in EPR. *J Magn Reson*. 2006;178:42-55. doi:10.1016/j.jmr.2005.08.013
23. Hanwell MD, Curtis DE, Lonie DC, Vandermeersch T, Zurek E, Hutchison GR. Avogadro: an advanced semantic chemical editor, visualization, and analysis platform. *J Chem*. 2012;4(1):17. doi:10.1186/1758-2946-4-17
24. Pritchard BP, Altarawy D, Didier B, Gibson TD, Windus TL. New basis set exchange: An open, up-to-date resource for the molecular sciences community. *J Chem Inf Model*. 2019;59:4814-4820. doi:10.1021/acs.jcim.9b00725
25. Frisch M. J., Trucks G. W., Schlegel H. B., et al. *Gaussian16*.
26. Fragoso A, Delgado R, Iranzo O. Copper (II) coordination properties of decapeptides containing three His residues: the impact of cyclization and Asp residue coordination. *Dalton Trans*. 2013;42:6182. doi:10.1039/C3DT32384F
27. Grasso G, Magrì A, Bellia F, Pietropaolo A, La Mendola D, Rizzarelli E. The copper (II) and zinc (II) coordination mode of HExxH and HxxEH motif in small peptides: The role of carboxylate location and hydrogen bonding network. *J Inorg Biochem*. 2014;130:92-102. doi:10.1016/j.jinorgbio.2013.09.021
28. Kállay C, Nagy Z, Várnagy K, Malandrinos G, Hadjiliadis N, Sóvágó I. Thermodynamic and structural characterization of the copper(II) complexes of peptides containing both histidyl and aspartyl residues. *Bioinorg Chem Appl*. 2007;2007:30394. doi:10.1155/2007/30394
29. Kállay C, Várnagy K, Malandrinos G, Hadjiliadis N, Sanna D, Sóvágó I. Thermodynamic and structural characterization of the macrochelates formed in the reactions of copper (II) and zinc (II) ions with peptides of histidine. *Inorg Chim Acta*. 2009;362:935-945. doi:10.1016/j.ica.2008.01.022
30. Matera A, Brasuń J, Cebrat M, Świątek-Kozłowska J. The role of the histidine residue in the coordination abilities of peptides with a multihistidine sequence towards copper (II) ions. *Polyhedron*. 2008;27:1539-1555. doi:10.1016/j.poly.2007.12.035
31. Brasun J, Matera-Witkiewicz A, Kamysz E, Kamysz W, Ołdziej S. The influence of the cyclopeptide sequence on its coordination abilities towards Cu (II). *Polyhedron*. 2010;29:1535-1542. doi:10.1016/j.poly.2010.01.029
32. Prenesti E, Daniele PG, Prencipe M, Ostacoli G. Spectrum–structure correlation for visible absorption spectra of copper (II) complexes in aqueous solution. *Polyhedron*. 1999;18:3233-3241. doi:10.1016/S0277-5387(99)00279-X
33. Kotynia A, Bielińska S, Kamysz W, Brasuń J. The coordination abilities of the multiHis-cyclopeptide with two metal-binding centers–potentiometric and spectroscopic investigation. *Dalton Trans*. 2012;41:12114. doi:10.1039/C2DT31224G
34. Lanza V, Milardi D, Di Natale G, Pappalardo G. Repurposing of copper (II)-chelating drugs for the treatment of neurodegenerative diseases. *Curr Med Chem*. 2018;25:525-539. doi:10.2174/0929867324666170518094404
35. Guerreiro JF, Gomes MAGB, Pagliari F, et al. Iron and copper complexes with antioxidant activity as inhibitors of the metastatic potential of glioma cells. *RSC Adv*. 2020;10(22):12699-12710. doi:10.1039/d0ra00166j

SUPPORTING INFORMATION

Additional supporting information can be found online in the Supporting Information section at the end of this article.

How to cite this article: Bortolus M, Kotynia A, Saielli G, et al. Detailed investigation of the binding abilities of the heterodomain of a multiHis cyclopeptide toward Cu(II) ions. *J Pept Sci*. 2024;30(6):e3568. doi:10.1002/psc.3568